



Article







Tradeoff Relations Between Intrinsic Concurrence and First-Order Coherence of Two-Qubit Cavity System: Qubit–Dipole Coupling and Decoherence Effects

Mostafa Hashem, A.-B. A. Mohamed, H. A. Hessian, Daniel Breaz, Ala Amourah and Sheza M. El-Deeb



Article

Tradeoff Relations Between Intrinsic Concurrence and First-Order Coherence of Two-Qubit Cavity System: Qubit–Dipole Coupling and Decoherence Effects

Mostafa Hashem ^{1,4} , A.-B. A. Mohamed ^{2,4} , H. A. Hessian ^{3,4} , Daniel Breaz ^{5,*} , Ala Amourah ^{1,6,*} 
and Sheza M. El-Deeb ⁷ 

- ¹ Mathematics Education Program, Faculty of Education and Arts, Sohar University, Sohar 311, Oman; mhassian@su.edu.om
 - ² Department of Mathematics, College of Science and Humanities, Prince Sattam bin Abdulaziz University, Al Kharj 11942, Saudi Arabia
 - ³ Department of Mathematics, Faculty of Science, Al-Baha University, Al-Baha 1988, Saudi Arabia; hasayed@bu.edu.sa
 - ⁴ Department of Mathematics, Faculty of Science, Assiut University, Assiut 71516, Egypt
 - ⁵ Department of Mathematics, 1 Decembrie 1918 University of Alba Iulia, 510009 Alba Iulia, Romania
 - ⁶ Applied Science Research Center, Applied Science Private University, Amman 11937, Jordan
 - ⁷ Department of Mathematics, College of Science, Qassim University, Buraydah 51452, Saudi Arabia; s.eldeeb@qu.edu.sa
- * Correspondence: dbreaz@uab.ro (D.B.); aamourah@su.edu.om (A.A.)

Abstract: An analytical exploration of the phase decoherence equation of two qubits interacting with a coherent field with dipole–dipole interaction is introduced. The study examines the tradeoff relationships between intrinsic concurrence and first-order coherence in the qubits–cavity system while considering the impacts of decoherence and the interactions among the qubits. We affirm that the relationship between intrinsic concurrence and first-order coherence is valid. Additionally, we demonstrate that the minimum limit of intrinsic concurrence is universally applicable, although the upper limit is typically not. These connections in Heisenberg models can provide a means by which to investigate how quantum resources are allocated in spins, potentially leading to future applications in quantum information processing. It is partially but not completely possible to control the tradeoff relations between intrinsic concurrence and first-order coherence of the two-qubit cavity system; this control might involve actions that influence the system and are reflected in intrinsic concurrence and first-order coherence.

Keywords: phase decoherence; concurrence; entanglement; open systems; dipole-dipole interaction; symmetry and tradeoff



Academic Editor: Calogero Vetro

Received: 2 February 2025

Revised: 24 February 2025

Accepted: 2 March 2025

Published: 7 March 2025

Citation: Hashem, M.; Mohamed, A.-B.A.; Hessian, H.A.; Breaz, D.; Amourah, A.; El-Deeb, S.M. Tradeoff Relations Between Intrinsic Concurrence and First-Order Coherence of Two-Qubit Cavity System: Qubit–Dipole Coupling and Decoherence Effects. *Symmetry* **2025**, *17*, 400. <https://doi.org/10.3390/sym17030400>

Copyright: © 2025 by the authors. Licensee MDPI, Basel, Switzerland. This article is an open access article distributed under the terms and conditions of the Creative Commons Attribution (CC BY) license (<https://creativecommons.org/licenses/by/4.0/>).

1. Introduction

In quantum mechanics, tradeoffs and symmetry are deeply interconnected. The preservation of symmetry in a system often constrains its evolution or measurement outcomes, as symmetry dictates certain conserved quantities such as energy or momentum and limits how the system can evolve over time. However, new tradeoffs emerge when symmetry is broken, such as in phase transitions or spontaneous symmetry breaking. These can involve competing physical properties, where optimizing one aspect of the system, such as coherence or entanglement, may require compromising others, such as stability or

precision. Thus, the interplay between symmetry and tradeoffs shapes the behavior and measurement possibilities of quantum systems.

In quantum information processing and quantum communication, the relationship between coherence and entanglement plays a pivotal role. Investigating the tradeoff between intrinsic concurrence and first-order coherence in a two-qubit cavity system that considers qubit–dipole coupling and decoherence effects can provide valuable insights into the fundamental limits of quantum information protocols and help in the development of more robust quantum technologies. In quantum mechanics, entanglement and coherence are two fundamental features of quantum states that are crucial for quantum information processing, communication, and computation. Although they are related in some ways, they represent distinct properties of a quantum system [1,2]. For pure two-qubit systems, there is indeed a complementary relationship between first-order coherence (*FOC*) and concurrence (*C*). While high coherence typically indicates a less entangled state, high entanglement often leads to a reduction in coherence [3,4]. Intrinsic concurrence (*IC*) is a critical measure for understanding the relationship between entanglement and coherence in two-qubit mixed states. Unlike standard concurrence, which is limited to pure states, *IC* extends the concept of entanglement to mixed states and shows the same complementary relationship with first-order coherence (*FOC*) that we see in pure states [5].

Furthermore, the authors of [6] have endeavored to connect *IC* and agreement through an inequality relationship without providing a strict mathematical demonstration. They assert that this is true for any generic two-qubit quantum system. Spin chains are robust and adaptable systems, and have gained considerable attention in quantum computing and quantum simulation because of their integrability, scalability, and diverse physical behavior. They serve as an ideal platform for studying entanglement, quantum correlations, and quantum phase transitions, offering great potential for building the next generation of quantum computers. As experimental techniques continue to improve and as new models for quantum error correction and fault tolerance are developed, spin chains are expected to play a central role in the development of scalable and practical quantum computing systems [7–12]. In [13], the authors studied the dynamics of quantum systems, focusing on how various Hamiltonians impact entanglement and coherence in multi-qubit states. They also examined engineering techniques that could enhance the efficiency and reliability of structural systems by using advanced materials and design principles. Furthermore, their research explored the statistical mechanics of complex systems, revealing insights into collective behavior and phase transitions in non-equilibrium environments as well as the relationship between classical and quantum mechanics in chaotic systems, particularly with regard to the influence of quantum correlations on information transfer in quantum cryptography. By discussing specific experimental systems such as superconducting qubits and trapped ions, their study provides concrete examples of how theoretical concepts such as coherence and entanglement are realized in practice. These systems demonstrate the practical challenges and innovations in manipulating quantum states and illustrate the implications of quantum dynamics in real-world applications. Highlighting such experimental platforms allows for a deeper understanding of the interplay between theory and experiment, enriching the overall discourse on quantum technologies [14].

Indeed, spin chains have become a crucial element in quantum mechanics, particularly for exploring quantum coherence and correlations. The Heisenberg model, which describes the interaction between spins in a quantum system, plays a significant role in this context [15–26]. Spin chain models provide fertile ground for studying quantum resources such as entanglement and coherence. The spin correlations within the chain can lead to powerful quantum phenomena that are central to advancing quantum technologies. These systems are also crucial for understanding the interplay between quantum mechanical

effects, many-body physics, and computational resources in quantum information science [27–30]. The two-qubit Heisenberg XYZ model represents one of the simplest yet most versatile spin chains, and has recently inspired the research community to quickly embrace the Heisenberg XYZ example [13–24]. The dissipative two-qubit Heisenberg XYZ model under the Dzyaloshinsky–Moriya interaction is a rich system for studying the effects of anisotropic spin interactions, relativistic corrections, and environmental dissipation on quantum correlations. All of this earlier research has motivated us to examine the tradeoff relationships for this model. Additionally, we investigate whether the suggested inequality relation is valid for this system and evaluate the tradeoff relationship to gain insights into the shared behavior of entanglement and coherence over time for different system parameters, such as the purity of the initially formed state, dipole–dipole interaction, quantity of photons, and attenuation parameter.

We organize the rest of this research paper in the following manner: in Section 2, we discuss the physical framework and its resolution, then provide a brief introduction to *C*, *FOC*, and *IC*; in Section 3, we examine the tradeoff relationships between *FOC* and *IC* along with the inequality relationship between *IC* and *C*; in Section 4, we employ the Heisenberg XYZ model to explore the tradeoff relationships between *C* and *IC*; finally, in Section 5, we showcase our results and findings before ultimately concluding the paper.

2. The Physical Model and Its Solution

We consider a model consisting of two qubits interacting resonantly with a coherent field, with dipole–dipole interaction taking place through via two-photon transitions. This model highlights the implications of photon interactions with two-level systems, emphasizing the differences between one-photon and two-photon cases. While one-photon processes allow for straightforward excitations and generation of entanglement, two-photon interactions lead to more complex dynamics that can be leveraged for enhanced control, nonlinearity, and robustness in quantum information applications. In the rotating-wave approximation, the Hamiltonian of the system is provided by

$$\begin{aligned} \hat{H} = & \omega \hat{a}^\dagger \hat{a} + \omega (\hat{\sigma}_1^z + \hat{\sigma}_2^z) + \lambda \sum_{i=1}^2 (\hat{a}^2 \sigma_i^+ + \hat{a}^{\dagger 2} \sigma_i^-) \\ & + \Omega (\sigma_1^+ \sigma_2^- + \sigma_1^- \sigma_2^+), \end{aligned} \quad (1)$$

where \hat{a} (\hat{a}^\dagger) denotes the annihilation (creation) operator of the resonant single-mode field, ω is atomic transition frequency and cavity frequency, λ is the coupling constant between qubits and cavity, the raising and lowering operators of the qubit i are $\hat{\sigma}_+^i$ and $\hat{\sigma}_-^i$ ($i = A, B$), respectively, and Ω is the qubit dipole–dipole coupling constant. Here, only the pure phase decoherence mechanism is considered. In this situation, the master equation governing the time evolution for the system is provided by [31,32]

$$\frac{d\rho(t)}{dt} = -i[H, \rho(t)] - \frac{\gamma}{2}[H, [H, \rho(t)]], \quad (2)$$

where γ is the phase decoherence parameter. The formal solution of the Equation (2) is provided by [33,34]

$$\rho(t) = \sum_{k=0}^{\infty} \frac{(\gamma t)^k}{k!} M^k(t) \rho(0) M^{\dagger k}(t), \quad (3)$$

where $M^k(t) = H^k e^{-iHt} e^{-\frac{\gamma t}{2} H^2}$ and where $\rho(0)$ is the density operator of the initial system. Analysis is confined to a four-dimensional subspace characterized by the most pertinent

states. We believe that this approach provides a meaningful representation of the system’s behavior under the studied conditions. In the space states $\{|1\rangle = |e_A e_B, n\rangle, |2\rangle = |e_A g_B, n + 2\rangle, |3\rangle = |g_A e_B, n + 2\rangle, |4\rangle = |g_A g_B, n + 4\rangle\}$, the used eigenstates $|\Psi_i^n\rangle$ of the Hamiltonian (1) are provided by

$$\begin{aligned} |\Psi_1^n\rangle &= C_{11}|1\rangle + C_{14}|4\rangle, \\ |\Psi_2^n\rangle &= C_{22}|2\rangle + C_{23}|3\rangle, \\ |\Psi_3^n\rangle &= C_{31}|1\rangle + C_{32}|2\rangle - C_{33}|3\rangle + C_{34}|4\rangle, \\ |\Psi_4^n\rangle &= C_{41}|1\rangle + C_{42}|2\rangle + C_{43}|3\rangle + C_{44}|4\rangle, \end{aligned} \tag{4}$$

where the coefficients C_{ij} satisfy the condition of the following eigenvalue problem: $\hat{H}|\Psi_m^n\rangle = E_m|\Psi_m^n\rangle$. Here, E_m are the corresponding eigenvalues:

$$\begin{aligned} E_1 &= \omega(n + 2), & E_2 &= \omega(n + 2) - \Omega, \\ E_{3(4)} &= \omega(n + 2) + \frac{\Omega}{2} \mp \frac{1}{2}\sqrt{\Omega^2 + 8(x^2 + y^2)} \end{aligned}$$

where $x = \lambda\sqrt{(n + 1)(n + 2)}$ and $y = \lambda\sqrt{(n + 3)(n + 4)}$. The explicit expression of the density matrix is provided by

$$\rho(t) = \sum_{mn} e^{-\frac{\gamma t}{2}(E_m - E_n)^2 - i(E_m - E_n)t} \langle \Psi_m | \rho(0) | \Psi_n \rangle |\Psi_m\rangle \langle \Psi_n|, \tag{5}$$

where $\hat{\rho}(0) = |e_A e_B\rangle \langle e_A e_B| \otimes |\alpha\rangle \langle \alpha|$ is the initial state of the entire system, i.e., the single-mode cavity field initially prepared in the coherent state,

$$|\alpha\rangle = \sum_{n=0}^{\infty} e^{-|\alpha|^2/2} \frac{\alpha^n}{\sqrt{n!}} |n\rangle, \tag{6}$$

while the two qubits are started in the pure excited state $\hat{\rho}^{AB}(0) = |e_A e_B\rangle \langle e_A e_B|$. This density matrix can be used to perform detailed study on the evolution of some measures of mixture and entanglement in the partitions of two dipole-coupled qubits interacting with a coherent cavity under decoherence effect.

3. Quantifiers of Tradeoff Relations of Quantum Information Resource

Here, we briefly review the concepts of first-order coherence (FOC), concurrence (C), and intrinsic concurrence (IC) in order to explore the dynamics of the tradeoff relations between the entanglement and coherence of the generated two-spin qubit states under intrinsic decoherence, spin-orbit interaction, and external magnetic field.

- **Intrinsic Concurrence**

The behaviors of the entanglement between the generated two spin qubit states are explored using the concurrence [35], provided by

$$C(t) = \max\{0, \sqrt{\lambda_1} - \sqrt{\lambda_2} - \sqrt{\lambda_3} - \sqrt{\lambda_4}\}, \tag{7}$$

where λ_i denotes the roots of the eigenvalues (organized in descending order, $\lambda_i > \lambda_{i+1}$) of the non-Hermitian matrix $R = D(t)\tilde{D}(t)$ depending on the spin-flipped density matrix $\tilde{D}(t) = [\tilde{d}_{ij}]$:

$$\tilde{d}_{ij} = \langle i | (\sigma^y \otimes \sigma^y) D^*(t) (\sigma^y \otimes \sigma^y) | j \rangle.$$

The initial pure two-spin qubit state has $C(t) = 0$, growing to a maximal state if $C(t) = 1$ and to a partially two-spin qubit state if $0 < C(t) < 1$. With the intrinsic concurrence [5] defined as above, for a two-qubit state $D(t)$, the intrinsic concurrence is defined as

$$C_I(t) = \sqrt{\text{Tr}[D(t)\tilde{D}(t)]}. \quad (8)$$

For a pure two-qubit state, the concurrence and intrinsic concurrence have the following dynamics. Due to $\text{Tr}[D(t)\tilde{D}(t)] = \sum_n \lambda_n$ [5], where λ_n ($n = 1, 2, 3, 4$) are the eigenvalues of the non-Hermitian matrix $R = D(t)\tilde{D}(t)$, the two-qubit concurrence is the lower bound of the intrinsic concurrence. This means that the dynamics of the two-spin Heisenberg qubit concurrence and the intrinsic concurrence allows the following inequality:

$$C(t) \leq C_I(t). \quad (9)$$

- **First-Order Coherence (FOC)**

The first-order coherence can be used to measure the generated coherence of a spin k -qubit state with the reduced density matrix $D^k(t)$ ($k = A, B$), where $D^A(t) = \text{Tr}_B[D(t)]$ and $D^B(t) = \text{Tr}_A[D(t)]$. The FOC of a k -qubit state is defined as

$$F_k(t) = \sqrt{2\text{Tr}[\rho_k(t)^2]} - 1. \quad (10)$$

Hence, considering all k -qubits independently, the first-order coherence measure of the whole two-qubit system can be provided by [36]

$$F_{AB}(t) = \sqrt{\frac{F_A(t) + F_B(t)}{2}}, \quad (11)$$

where the two-qubit first-order coherence satisfies $0 \leq F_{AB}(t) \leq 1$.

- For a general two-qubit state such as $D(t)$, the complementary relation between the intrinsic concurrence and first-order coherence is introduced as follows:

$$F_{AB}^2(t) + C_I^2(t) = \text{Tr}[D^2(t)]. \quad (12)$$

This means that for a closed two-qubit system there is a mutual transformation relationship between its first-order and intrinsic concurrence, while for an open two-qubit system the tradeoff relations between the two-qubit nonlocal correlation and the first-order coherence depends on the purity degree $P(t) = \text{Tr}[D^2(t)]$ of the whole two-qubit system, which is measured by the whole linear entropy equaling to $1 - \text{Tr}[D^2(t)]$.

4. Two-Spin Heisenberg XYZ-Qubits Dynamics

Figure 1 shows the generation of the concurrence (C) and intrinsic concurrence (IC) under the intrinsic decoherence effect along with the degradation of the first-order coherence (FOC) in two-qubit states due to atom–cavity interactions without atom–atom interactions. For this, the two atoms are initially considered in the pure upper states $|1_A\rangle \otimes |1_B\rangle$, where the initial density matrix has no entanglement, i.e., the concurrence and intrinsic concurrence start with zero values ($C(0) = C_I(0) = 0$) and the considered quantifiers have maximal coherence ($F_{AB}(0) = 1$) and purity ($P(0) = 1$). Below, we show the FOC, C , and IC dynamics and total mixedness of two non-interacting qubits starting with pure state $|1_A\rangle \otimes |1_B\rangle$ inside a coherent field cavity with $\alpha = 2$ photons under different decoherence effects γ/λ : (a) shows $\gamma = 0$, (b) shows $\gamma = 0.001\lambda$, and (c) shows $\gamma = 0.015\lambda$.

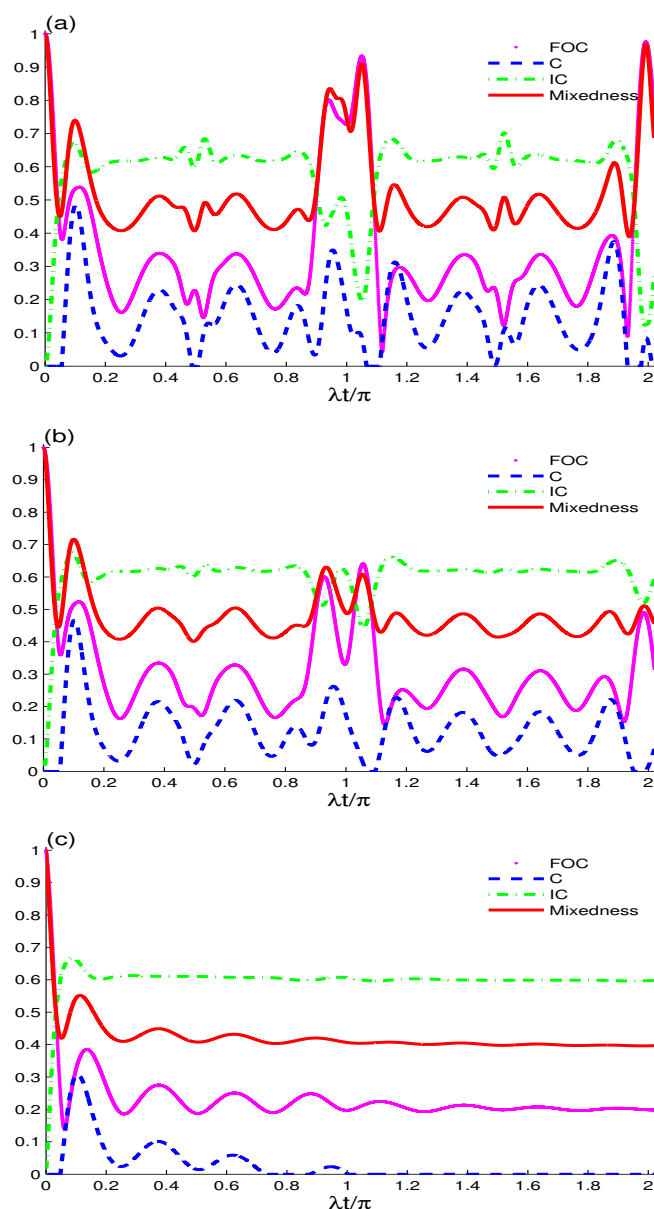


Figure 1. Dynamics of FOC, C, IC, and total mixedness of two non-interacting qubits starting with pure state $|e_A\rangle \otimes |e_B\rangle$ inside a coherent field cavity with $\alpha = 2$ photons under different decoherence effects γ/λ : (a) $\gamma = 0$, (b) $\gamma = 0.001\lambda$, and (c) $\gamma = 0.015\lambda$.

By comparing Figures 1 and 2a it can be seen that the evolution of FOC, C, IC, and total mixedness follows roughly the same quantitative behavior, with different amplitude values for each. Based on the context, these terms might refer to measures of concentration, distribution, or diversity in a system. To better clarify this, we can expand on the potential interpretation. In Figure 2a, there is doubling of the oscillation periods in the interval $[0, 2\pi]$ with momentum and interference from oscillations, whereas the total mixedness (indicated by the red line) represents the upper bound of IC. It can be observed that for the most part the total mixedness and FOC are above the IC; however, in some places the green plot outperforms the red plot, indicating that $\text{mixedness}, \text{FOC} < \text{CI}$ instead of $\text{CI} < \text{mixedness}, \text{FOC}$. Therefore, we can conclude that while the lower bound of IC stated in Equation (9) is universally true, the upper bound is generally not (see Figures 1 and 2a). Next, we can investigate the effect of the phase decoherence for this bound. Figures 1 and 2b show the plots for these functions when $\gamma = 0.001\lambda$. Again, we can see that $\text{mixedness}, \text{FOC} < \text{CI}$ for some specific intervals. Therefore, it can be confirmed that the

hypothesized upper bound of IC is not always met. Here, we notice that the maximum values of $mixedness$ and C decrease with the entry of γ , while the values of FOC and IC remain unchanged. Figures 1 and 2c show the coherent and evenly coherent states with the development of time and increase in the value of the gamma decay. It can be noticed that the amplitude values of IC , FOC and $mixedness$ are confined between $0.6 < CI < 0.7$, $0.4 < mixedness < 0.5$, and $0.2 < FOC < 0.3$, while C turns to zero when $t \geq \pi$. Thus, it can be concluded that the gamma decay effect leads to $mixedness < FOC < CI < C \rightarrow 0$. After a certain γ is reached, the concurrence vanishes; however, the FOC , IC , and total mixedness still exist.

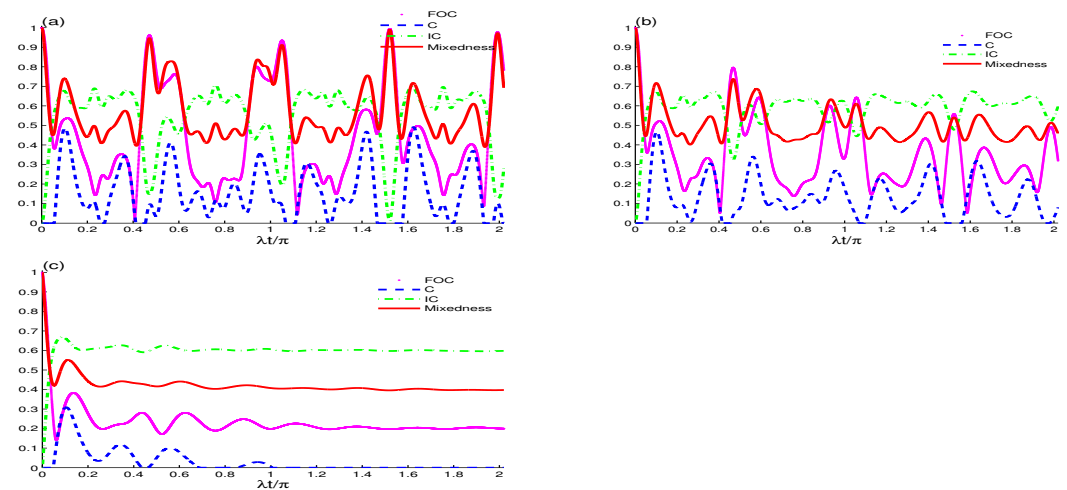


Figure 2. Same as Figure 1 except that the two non-interacting qubits are inside a cavity filled by an evenly coherent field.

We now examine the impact of the qubit dipole–dipole coupling constant interaction on the previously discussed quantifiers as well as the accompanying complementary tradeoff relationship. Figures 3 and 4 demonstrate the collective decoherence-free dynamics for each of FOC , C , IC , and total mixedness as functions of t for different fixed values of γ and with interacting qubits $\Omega = 30$. In Figures 3 and 4a, where $\gamma = 0$, it can be concluded that the evolution of the initial state for FOC , C , IC , and total mixedness retains separability at $t = 0$ for all ensuing instances of $t > 0$. As a result, dipole–dipole interaction takes place. Furthermore, our findings show that increasing the strength of the Ω interaction results in the creation of entanglement. Additionally, it has been demonstrated that the behaviors of entanglement (captured by C), coherence (captured by FOC), intrinsic concurrence (captured by IC), and total mixedness are constant at any moment regardless of the intensity of the Ω interaction. This suggests that the Ω interaction cannot induce or enhance either coherence or entanglement in this scenario. In Figures 3 and 4b, where $\gamma = 0.001\lambda$, it is evident that the Ω interaction creates an additional wiggling or ripple effect, influencing not only C but also IC , FOC , and $mixedness$. We also note that, as expected, increasing γ leads to a decrease in the maximum values for all measures. A similar pattern is evident for $\gamma = 0.015\lambda$ in Figures 3 and 4c, except that now entanglement (represented by C) and coherence (represented by FOC) are mostly zero. Although the Ω interaction cannot increase the maximum value of entanglement, it decreases the minimum value of concurrence. Therefore, it can be said that the presence of dipole–dipole interactions can be used to entangle qubits. By controlling the dipole–dipole coupling strength and phase decoherence parameter γ , it is possible to generate entangled states, which are the foundation of many quantum algorithms and protocols. We anticipate that as the value of the Ω interaction increases, C will attempt to replicate the changes observed in C as the value of γ rises, albeit not perfectly. Furthermore, an increase in the Ω interaction

leads to a rise in the average oscillation frequency of FOC , C , IC , and overall mixedness. In order to study this system more deeply and incorporate the concept of tradeoffs, we now investigate the effect of increasing the number of photons $\alpha = 5$ with the absence in the decoherence effect $\gamma = 0.0$, as shown in Figure 5a,b. It can be observed that C and FOC behave identically and that increasing the value of the $\alpha = 5$ interaction significantly increases the oscillation frequency. Generally speaking, given that the initial state is an entangled one, we can assert that an increase in the number of photon interactions leads to a rise in the oscillation frequencies of FOC , C , and IC . Furthermore, it is evident that the lower bound of IC , as outlined in Equation (9), is upheld effectively. Figure 6a,b shows the result of increasing the dipole–dipole coupling in a two-qubit cavity system to $\Omega = 60$. As can be seen, this increase causes a significant change in the maximum values of all measures (FOC , C , IC , and total mixedness), resulting in a significant decrease. Additionally, even in the case of non-zero decoherence, when including the lower bound of IC as provided in Equation (9), the tradeoff relation is preserved entirely strictly. At $t = 0$, the IC and C have the same values because the initialized state is maximally entangled (as shown in Figure 7a,b with $\gamma = 0.01\lambda$). On the other hand, decoherence alters and gradually lowers their values. Likewise, with greater values of γ , the entanglement survival time before the full entanglement death is reduced. Lastly, Equation (12), which is a recently proposed conservation relation, represents the tradeoff relation between FOC and IC . There is an inherent tradeoff between entanglement (concurrence) and coherence in the system; in this case, while strong coupling to the cavity field can enhance entanglement (concurrence), this can lead to increased decoherence due to coupling with the environment (see Figure 7a,b). As decoherence increases, the system loses both its coherence and entanglement. Thus, the system may experience a reduction in concurrence as decoherence rates increase. Conversely, in a system with low coupling to the field (or low decoherence), the qubits can maintain higher coherence and entanglement. However, without sufficient coupling, the entanglement between the qubits may be weak, leading to lower concurrence.

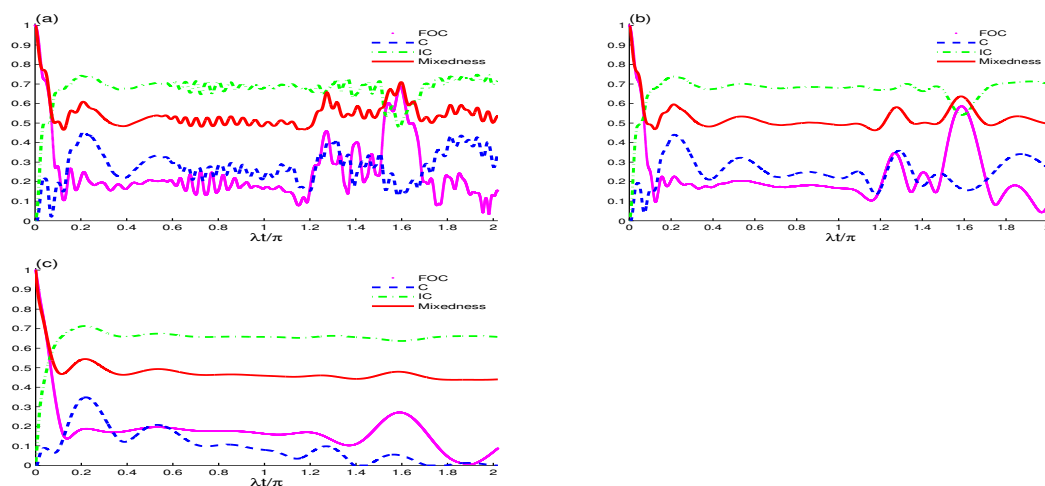


Figure 3. Same as Figure 1 except for two interacting qubits $\Omega = 30\lambda$. (a) $\gamma = 0$, (b) $\gamma = 0.001\lambda$, and (c) $\gamma = 0.015\lambda$.

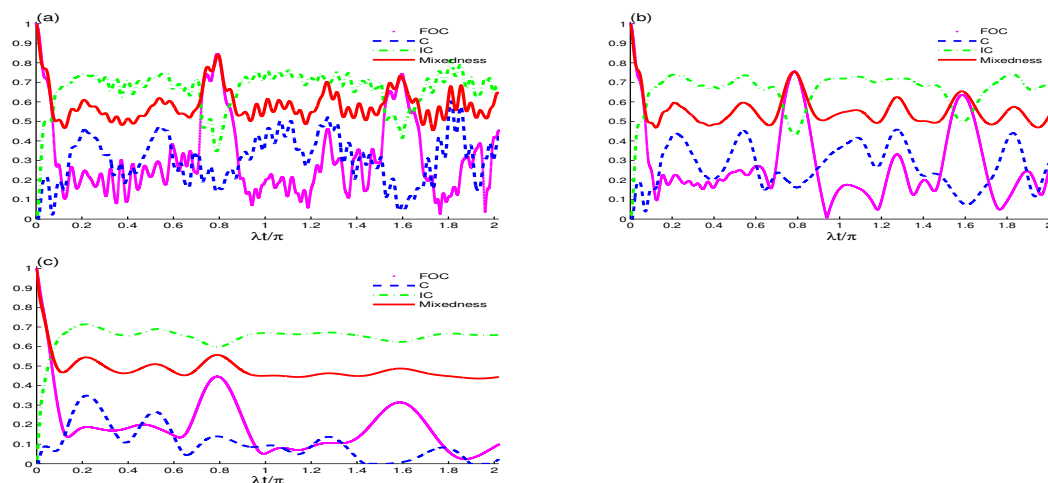


Figure 4. Same as Figure 2, except for two non-interacting qubits $\Omega = 30\lambda$.

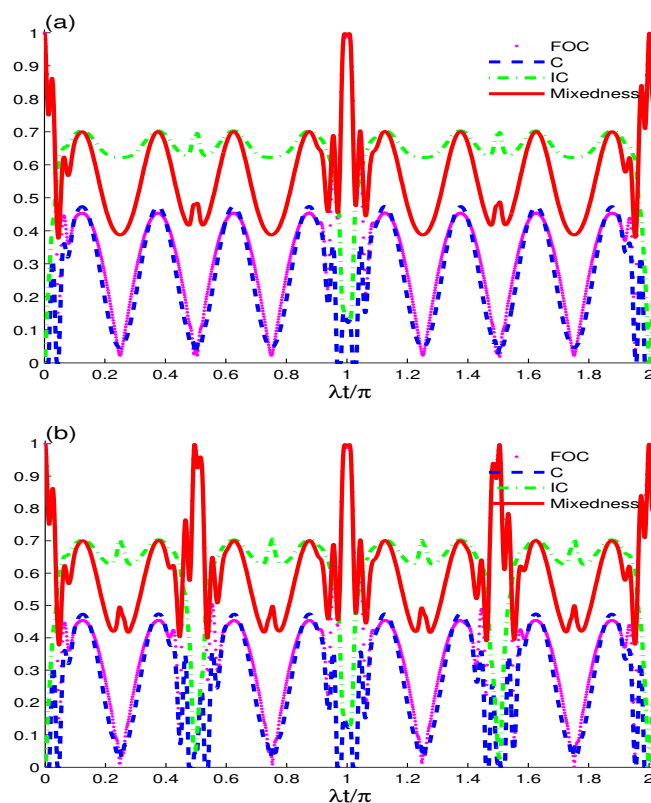


Figure 5. Dynamics of FOC, C, IC, and total mixedness for two non-interacting qubits starting with pure state $|e_A\rangle \otimes |e_B\rangle$, $\alpha = 5$ photons, and absence of the decoherence effect $\gamma = 0.0$ inside (a) a coherent field cavity and (b) an evenly coherent field cavity.

The damped oscillatory behavior in the dynamics of concurrence and first-order coherence arises from the interplay between coherent quantum interactions and weak decoherence when the phase decoherence parameter γ is small. In a system of coupled two-level atoms interacting with a cavity field, coherence from atomic state superpositions leads to Rabi-like oscillations. Despite small γ indicating weak decoherence, which typically suggests monotonic damping, the strong coupling allows significant oscillations to persist, resulting in a damped oscillatory pattern instead of simple exponential decay. This behavior reflects the interplay of preserved coherence and the gradual influence of decoherence, resulting in a complex dynamic that illustrates the resilience of quantum correlations amid environmental interactions.

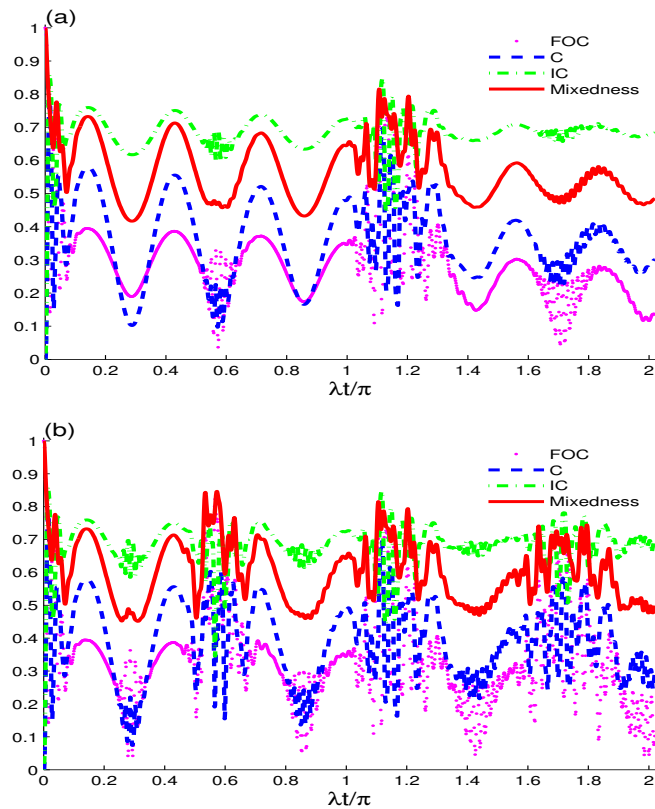


Figure 6. Same as Figure 5, except for two interacting qubits $\Omega = 60\lambda$.

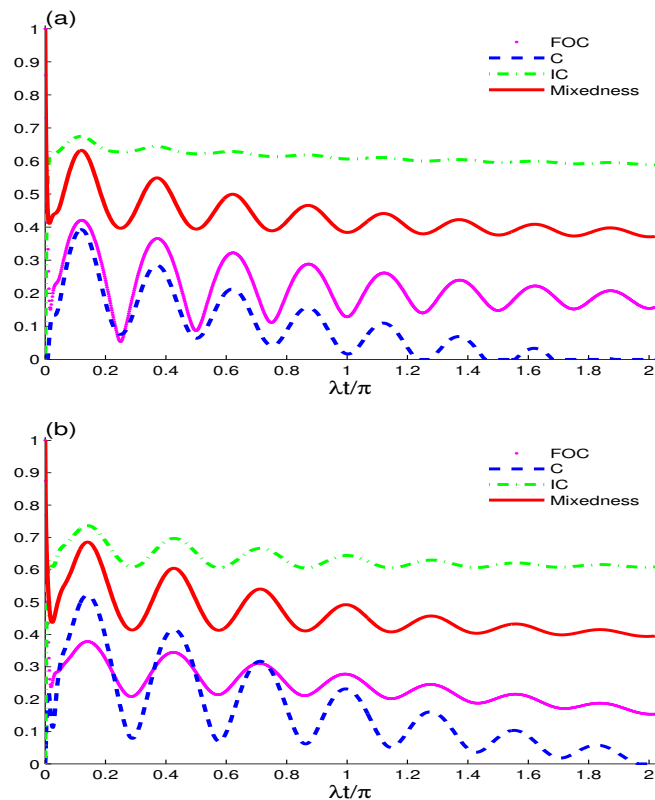


Figure 7. Same as Figures 5a and 6a, except with the decoherence effect $\gamma = 0.01\lambda$.

5. Conclusions

In this paper, we have investigated the situation of two dipole-coupled qubits interacting with a coherent cavity field in the presence of phase decoherence. The inherent relations

between FOC , C , IC , and total mixedness can help us to better understand how quantum resources are distributed and how entanglement and coherence affect each other. The universal tradeoff between these measures underlines a fundamental aspect of quantum systems, making the study of their relations essential for advancing both theoretical and practical applications in quantum technology. This provides strong motivation to study and analytically explore the master equation for this physical model. In particular, one of our strongest interests in this paper has been to study the dynamics of FOC , C , IC , and total mixedness for two interacting qubits starting in a pure state inside a coherent field cavity and under decoherence effects. The tradeoff relation, which is universal for any arbitrary two-qubit states, indicates that mixedness and FOC decrease as the level of IC increases (and vice versa) when the coherence effect is absent or weak. However, this does not occur with increasing decay or when dipole–dipole interaction occurs, as the amplitude of IC becomes higher than those of mixedness and FOC with the development of time. By controlling the dipole–dipole coupling strength and the phase decoherence parameter γ , it is possible to generate entangled states, which are the foundation of many quantum algorithms and protocols. The increase in the number of interacting photons is responsible for increasing the oscillation frequency of FOC , C , and IC , provided that the initially established state is the entangled state. There is an inherent tradeoff between entanglement (concurrence) and coherence in the system; in this case, strong coupling to the cavity field can enhance entanglement (concurrence), but this can also lead to increased decoherence due to coupling with the environment. By studying the measures of FOC , C , IC , and total mixedness as well as the effects of dipole–dipole interaction, decoherence, and the number of photons, it is possible to partially but not completely control the tradeoff relations between intrinsic concurrence and first-order coherence of a two-qubit cavity system. Understanding these phenomena requires rigorous analysis of specific quantum states and their dynamics, challenging existing models and prompting the need for more robust frameworks in real-world applications of quantum mechanics. This control might involve actions that influence the system and that are reflected in the measures of FOC , C , IC , and total mixedness. We checked the validity of the tradeoff relation between IC and FOC and the inequality relation between IC and C , confirming that the tradeoff relation between IC and FOC holds tightly in the given model, that is, $F_{AB}^2(t) + C_I^2(t) = Tr[D^2(t)]$. However, the upper bound of the inequality between IC and C , i.e., $C(t) \leq C_I(t)$, generally does not hold. Therefore, the dynamics exhibit damped oscillations, revealing the intricate balance between coherence and decoherence in quantum systems.

Author Contributions: Conceptualization, M.H. and A.-B.A.M.; methodology, H.A.H., D.B. and A.A.; validation, M.H., H.A.H. and D.B.; formal analysis, S.M.E.-D.; investigation, M.H., A.-B.A.M. and A.A.; writing—original draft preparation, M.H. and A.-B.A.M.; writing—review and editing, D.B., A.A. and S.M.E.-D.; supervision, M.H. All authors have read and agreed to the published version of the manuscript.

Funding: This research received no external funding.

Data Availability Statement: Data are contained within the article.

Conflicts of Interest: The authors declare no conflicts of interest.

References

1. Nielsen, M.A.; Chuang, I.L. *Quantum Computation and Quantum Information*; Cambridge University Press: Cambridge, UK, 2003.
2. Hu, M.-L.; Hu, X.Y.; Wang, J.C.; Peng, Y.; Zhang, Y.-R.; Fan, H. Quantum coherence and geometric quantum discord. *Phys. Rep.* **2018**, *762–764*, 1–100. [[CrossRef](#)]
3. Dong, D.-D.; Song, X.-K.; Fan, X.-G.; Ye, L.; Wang, D. Complementary relations of entanglement, coherence, steering, and Bell nonlocality inequality violation in three-qubit states. *Phys. Rev. A* **2023**, *107*, 052403. [[CrossRef](#)]

4. Dong, D.-D.; Wei, G.-B.; Song, X.-K.; Wang, D.; Ye, L. Unification of coherence and quantum correlations in tripartite systems. *Phys. Rev. A* **2022**, *106*, 042415. [[CrossRef](#)]
5. Fan, X.-G.; Sun, W.-Y.; Ding, Z.-Y.; Ming, F.; Yang, H.; Wang, D.; Ye, L. Universal complementarity between coherence and intrinsic concurrence for two-qubit states. *New J. Phys.* **2019**, *21*, 093053. [[CrossRef](#)]
6. Zhou, A.-L.; Wang, D.; Fan, X.-G.; Ming, F.; Ye, L. Mutual restriction between concurrence and intrinsic concurrence for arbitrary two-qubit states. *Chin. Phys. Lett.* **2020**, *37*, 110302. [[CrossRef](#)]
7. Meier, F.; Levy, J.; Loss, D. Quantum computing with spin cluster qubits. *Phys. Rev. Lett.* **2003**, *90*, 047901. [[CrossRef](#)]
8. Yu, H.; Zhao, Y.; Wei, T.-C. Simulating largesize quantum spin chains on cloud-based superconducting quantum computers. *Phys. Rev. Res.* **2023**, *5*, 013183. [[CrossRef](#)]
9. Boixo, S.; Rnnow, T.F.; Isakov, S.V.; Wang, Z.; Wecker, D.; Lidar, D.A.; Martinis, J.M.; Troyer, M. Evidence for quantum annealing with more than one hundred qubits. *Nat. Phys.* **2014**, *10*, 218–224. [[CrossRef](#)]
10. Harris, R.; Sato, Y.; Berkley, A.J.; Reis, M.; Altomare, F.; Amin, M.; Boothby, K.; Bunyk, P.; Deng, C.; Enderud, C.; et al. Phase transitions in a programmable quantum spin glass simulator. *Science* **2018**, *361*, 162–165. [[CrossRef](#)]
11. Labuhn, H.; Barredo, D.; Ravets, S.; De Leseleuc, D.; Macri, T.; Lahaye, T.; Browaeys, A. Tunable two dimensional arrays of single Rydberg atoms for realizing quantum ising models. *Nature* **2016**, *534*, 667–670. [[CrossRef](#)]
12. Kikuchi, Y.; Keever, C.M.; Coopmans, L.; Lubasch, M.; Benedetti, M. Realization of quantum signal processing on a noisy quantum computer. *npj Quantum Inf.* **2023**, *9*, 93. [[CrossRef](#)]
13. Mohamed, A.-B.A.; Rmili, H.; Omri, M.; Abdel-Aty, A.H. Two-qubit quantum nonlocality dynamics induced by interacting of two coupled superconducting flux qubits with a resonator under intrinsic decoherence. *Alex. Eng. J.* **2023**, *77*, 239–246. [[CrossRef](#)]
14. Xu, K.; Wang, S.S.J.; Turner, J.S.E.F.; Kjaergaard, M.; Hartmann, J.I.A.M.H.; Gambetta, J.M. Controlled Environment for Superconducting Qubits and Implementation of Quantum Logic Gates. *Phys. Rev. Lett.* **2022**, *128*, 150501. [[CrossRef](#)]
15. Kuzmak, A. Entanglement of the isingheisenberg diamond spin-cluster in evolution. *J. Phys. A Math. Theor.* **2023**, *56*, 165302. [[CrossRef](#)]
16. Zhang, Y.; Kang, G.; Yi, S.; Xu, H.; Zhou, Q.; Fang, M. Relationship between quantum-memoryassisted entropic uncertainty and steered quantum coherence in a two-qubit x state. *Quantum Inf. Process.* **2023**, *22*, 114. [[CrossRef](#)]
17. Zhang, Y.; Zhou, Q.; Fang, M.; Kang, G.; Li, X. Quantum-memory-assisted entropic uncertainty in twoqubit Heisenberg XYZ chain with Dzyaloshinskii-Moriya interactions and effects of intrinsic decoherence. *Quantum Inf. Process.* **2018**, *17*, 326. [[CrossRef](#)]
18. Yurischev, M.A. On the quantum correlations in two-qubit XYZ spin chains with Dzyaloshinsky Moriya and Kaplan-Shekhtman-Entin-Wohlman-Aharony interactions. *Quantum Inf. Process.* **2020**, *19*, 336. [[CrossRef](#)]
19. Park, D. Thermal entanglement and thermal discord in two-qubit Heisenberg XYZ chain with Dzyaloshinskii Moriya interactions. *Quantum Inf. Process.* **2019**, *18*, 172. [[CrossRef](#)]
20. Aldosari, F.M.; Alsahli, A.M.; Mohamed, A.-B.A.; Rahman, A.U. Control of quantum-memory induced by generated thermal XYZ-Heisenberg entanglement: y -component DM interaction. *Ann. Phys.* **2023**, *535*, 2300094. [[CrossRef](#)]
21. Yurischev, M.A.; Haddadi, S. Local quantum Fisher information and local quantum uncertainty for general X states. *Phys. Lett. A* **2023**, *476*, 128868. [[CrossRef](#)]
22. Benabdallah, F.; El Anouz, K.; Rahman, A.U.; Daoud, M.; El Allati, A.; Haddadi, S. Witnessing quantum correlations in a hybrid qubit-qutrit system under intrinsic decoherence. *Fortschritte Phys.* **2023**, *71*, 2300032. [[CrossRef](#)]
23. Zidan, N.; Rahman, A.U.; Haddadi, S.; Czerwinski, A.; Haseli, S. Local quantum uncertainty and quantum interferometric power in an anisotropic two-qubit system. *Universe* **2023**, *9*, 5. [[CrossRef](#)]
24. Mohamed, A.-B.A.; Khedr, A.N.; Haddadi, S.; Rahman, A.U.; Tammam, M.; Pourkarimi, M.R. Intrinsic decoherence effects on nonclassical correlations in a symmetric spin orbit model. *Results Phys.* **2022**, *39*, 105693. [[CrossRef](#)]
25. Hashem, M.; Mohamed, A.-B.A.; Haddadi, S.; Khedif, Y.; Pourkarimi, M.R.; Daoud, M. Bell nonlocality, entanglement, and entropic uncertainty in a Heisenberg model under intrinsic decoherence: DM and KSEA interplay effects. *Appl. Phys. B* **2022**, *128*, 87. [[CrossRef](#)]
26. Tacchino, F.; Chiesa, A.; Carretta, S.; Gerace, D. Quantum computers as universal quantum simulators: State-of-the-art and perspectives. *Adv. Quantum Technol.* **2020**, *3*, 1900052. [[CrossRef](#)]
27. Wang, A.; Zhang, J.; Li, Y. Error-mitigated deepcircuit quantum simulation of open systems: Steady state and relaxation rate problems. *Phys. Rev. Res.* **2022**, *4*, 043140. [[CrossRef](#)]
28. Shahbeigi, F.; Karimi, M.; Karimipour, V. Simulating of X-states and the two-qubit XYZ Heisenberg system on IBM quantum computer. *Phys. Scr.* **2022**, *97*, 025101. [[CrossRef](#)]
29. Wu, Q.; Shi, Y.; Zhang, J. Qubits on programmable geometries with a trapped-ion quantum processor. *arXiv* **2023**, arXiv:2308.10179.
30. Vandersypen, L.M.; Eriksson, M.A. Quantum computing with semiconductor spins. *Phys. Today* **2019**, *72*, 38–45. [[CrossRef](#)]
31. Gardiner, C.W. *Quantum Noise*; Springer: Berlin, Germany, 1991.
32. Milburn, G.J. Intrinsic decoherence in quantum mechanics. *Phys. Rev. A* **1991**, *44*, 5401. [[CrossRef](#)]

33. Moya-Cessa, H.; Buzek, V.; Kim, M.S.; Knight, P.L. Intrinsic decoherence in the atom-field interaction. *Phys. Rev. A* **1993**, *48*, 3900. [[CrossRef](#)] [[PubMed](#)]
34. Xu, J.-B.; Zou, X.-B. Dynamic algebraic approach to the system of a three-level atom in the Λ configuration. *Phys. Rev. A* **1999**, *60*, 4743. [[CrossRef](#)]
35. Wootters, W.K. Entanglement of Formation of an Arbitrary State of Two Qubits. *Phys. Rev. Lett.* **1998**, *80*, 2245. [[CrossRef](#)]
36. Svozilik, J.; Vallés, A.; Peřina, J.; Torres, J.P. Revealing Hidden Coherence in Partially Coherent Light. *Phys. Rev. Lett.* **2015**, *115*, 220501. [[CrossRef](#)] [[PubMed](#)]

Disclaimer/Publisher's Note: The statements, opinions and data contained in all publications are solely those of the individual author(s) and contributor(s) and not of MDPI and/or the editor(s). MDPI and/or the editor(s) disclaim responsibility for any injury to people or property resulting from any ideas, methods, instructions or products referred to in the content.